

The backrub motion: How protein backbone shrugs when a sidechain dances

Ian W. Davis, W. Bryan Arendall III, David C. Richardson, Jane S. Richardson*

Department of Biochemistry, Duke University, Durham, NC 27710-3711, USA

* corresponding author: jsr@kinemage.biochem.duke.edu

Summary

Surprisingly, the frozen structures from ultra-high-resolution protein crystallography reveal a prevalent but subtle mode of local backbone motion coupled to much larger, 2-state changes of sidechain conformation. The "backrub" is a previously unrecognized small-amplitude motion that appears to be an influential and common type of local plasticity in protein backbone. Concerted reorientation of two adjacent peptides swings the central sidechain perpendicular to chain direction, changing accessible sidechain conformations with flanking structure undisturbed. Alternate conformations in sub-1Å crystal structures show backrub motions for 2/3 of significant C β shifts and 3% of the total residues in these proteins (126/3882), accompanied by 2-state changes of sidechain rotamer. The BACKRUB modeling tool is effective in crystallographic rebuilding. For homology modeling or protein redesign, backrubs can provide realistic small perturbations to rigid backbones. For large sidechain changes in protein dynamics or single mutations, backrubs allow backbone accommodation while maintaining H-bonds and ideal geometry.

Keywords

coupled backbone-sidechain motion / alternate conformations / atomic resolution / kinemage graphics / backbone dynamics / protein design / homology modeling / protein evolution

Running Title

The backrub motion

Introduction

A large body of experimental dynamics data, especially nuclear magnetic resonance (NMR) measurements (Cavanagh et al., 1996; Wuthrich, 1986), shows that a protein molecule in solution is quite mobile, at a range of size and time scales. A major driving force for residue-scale mobility is the constant bombardment by solvent and other molecules, felt especially by surface sidechains which dance between favorable conformations (rotamers) under that bombardment and transfer some of those forces to their local backbone. Indeed, sidechains are seen to be more highly mobile than backbone by NMR (Kay, 2005; Palmer, 2004), and surface sidechain mobility is also evident in crystallographic electron density maps even when it is not explicitly modeled. Analogous structural changes occur over the much longer evolutionary time scale, where the primary event is a sequence mutation (i.e., sidechain substitution) but the effects propagate to cause shifts in backbone conformation. The combination of exquisite packing (Word et al., 1999a) and relaxed conformations (Lovell et al., 2003; Lovell et al., 2000) in protein cores, along with the degeneracy of permissible sequences (Gassner et al., 1996; Lim and Sauer, 1989; Munson et al., 1994), implies that the backbone must exhibit low-energy, localized modes of change that co-adapt sidechain and backbone conformations to the new local structural requirements of sequence changes.

In either the dynamic or evolutionary case, however, even something as “simple” as backbone accommodation to local sequence or rotamer change is surprisingly difficult to model accurately. For large-scale backbone motions, various methods can produce approximate results close enough to be of practical utility: molecular dynamics (Karplus and McCammon, 2002; Lipari et al., 1982), elastic networks (Bahar et al., 1997), inverse kinematics (van den Bedem et al., 2005), iterative simulation of fragment combinations (Rohl et al., 2004), and systematic secondary-structure deformations (Qian et al., 2004). However, accurate prediction of local backbone changes has been elusive, which is a problem for several fields. Crystal structures of mutant proteins show conclusively that small backbone rearrangements are indeed very common (Baldwin et al., 1993; Matthews, 1995), but energy calculations are still unable to predict those changes accurately. The detailed interpretation of backbone order parameters measured by NMR dynamics is hampered by the lack of reliable alternative models for local backbone motion. The notable successes of protein redesign (Dahiyat and Mayo, 1997; Desjarlais and Handel, 1995; Looger et al., 2003) mostly depend on limitation to a completely rigid backbone scaffold taken from a known natural structure. Similarly, homology modeling (Tramontano and Morea, 2003) generally works best if the core backbone of the template structure is left unchanged, although we know that the backbone will in fact accommodate somewhat (Mooers et al., 2003). Modeling of small local backbone motion is usually done either with molecular dynamics or with a set of pre-defined geometrical "moves" such as peptide flips or crankshaft ϕ/ψ motions (Fadel et al., 1995). Problems with these approaches include allowing unrealistic backbone motions (Hu et al., 2003), holding fixed the sidechains and surrounding structure, and not explicitly

considering correlated motions of adjacent peptides or coupling with changes of sidechain conformation.

Our attention was first drawn to backbone-sidechain coupling when manipulating brass “Kendrew” models, where a correlated twist of adjacent peptides is effective for swinging C α -C β bonds up perpendicular to a β sheet. Similar shifts of C β directionality were invoked to account for altered near-neighbor packing of aromatic residues in our protein design work (Richardson et al., 1992). When the rebuilding of backward-fit sidechains in crystal structures required adjustment of the C α -C β direction (Richardson et al., 2003), we investigated plausible backbone motions and prototype software tools to accomplish those changes ((Noonan et al., 2004) and Methods). These small backbone and C β shifts have been an important factor in the success of our structure-improvement methods (Arendall et al., 2005). Until now, however, there was no direct evidence as to whether this motion actually occurs in the molecules themselves.

The current study describes the small-scale, local “backrub” motion; shows that the backrub is the most common local backbone change seen in ultra-high-resolution protein structures; describes the BACKRUB algorithm for modeling such shifts; and shows that this low-energy, small-amplitude concerted shift of the backbone atoms in two successive peptides is coupled to much larger-scale, two-state change of conformation for the central sidechain. This constitutes one important example of a new paradigm of local backbone motion that is both demonstrably realistic and explicitly sidechain-coupled.

Methods

Survey of ultra-high-resolution crystal structures: The database consisted of all proteins with deposited structure factors at $\leq 0.9\text{\AA}$ resolution available in the Protein Data Bank (Berman et al., 2000) as of May 2004, excluding duplicates at $\geq 50\%$ identity and short peptides with unusual amino acids. The resulting 19 proteins, containing 3882 residues, are listed by resolution in Table 1. All 19 structure determinations used synchrotron data collected at cryogenic temperatures and refined anisotropic B-factors. Phasing methods varied, but all except two were refined with ShelXL (Schneider and Sheldrick, 2002).

Sidechain rotamers are defined and named as for the Penultimate rotamer library (Lovell et al., 2000); “p”, “t”, and “m” in those names refer to χ angles near $+60^\circ$, 180° , and -60° respectively. Structure analysis and creation of display files was done on-line in the MOLPROBITY web service at <http://kinemage.biochem.duke.edu/> (Davis et al., 2004; Richardson et al., 2003). If not already present, all hydrogen atoms were added and optimized with REDUCE (Word et al., 1999b), but without flips of Asn/Gln/His orientation. All-atom contacts were calculated by PROBE (Word et al., 1999a), giving scores and displays for H-bonds, van der Waals contacts, and the rare instances of bad steric overlap in these high-accuracy structures. Kinemage 3D display files were made with the “multi-criterion” function in MOLPROBITY, which highlights alternate conformations, poor rotamers (Lovell et al., 2000), Ramachandran outliers (Lovell et al., 2003), and serious all-atom clashes (overlaps $\geq 0.4\text{\AA}$), with user-controllable extra detail.

The multi-criterion kinemages were viewed in the KiNG Java display program (Davis et al., 2004), along with $2F_o-F_c$ and F_o-F_c maps obtained from the Electron Density Server at <http://eds.bmc.uu.se> (Kleywegt et al., 2004).

For each protein, Table 1 lists the number of residues for which an alternate conformation was defined for at least one atom (569/3882 residues total, or 15%). Alternate conformations involving concerted movement for the backbone of two or more neighboring residues were not analyzed in this study; omitting those 24 cases (93 residues) gives the 476 single-residue alternates. All single residues with alternate conformations defined for the C β atom (404 residues) are potential candidates for backbone movement, because a true shift of C β means the backbone must have moved, although small backbone changes are often modeled only as anisotropic B factors. After a preliminary survey, it was determined that a shift of at least 0.2Å in C β position was necessary in order to draw unambiguous conclusions about the specific changes in backbone conformation. 200 single-residue alternates had C β shifts $\geq 0.2\text{\AA}$ (see Table 1). 34 of them were omitted; half were not relevant because both sidechain conformations could actually be well fit from a single ideal C β position, implying no backbone motion (e.g. 1N9B Leu30, shown in the Supplement; 1SSX Met213), while for the others electron density for the lower-occupancy conformation was visible for too few atoms or too poorly-shaped to allow reliable inferences about the geometry of backbone changes (e.g. 1GWE Val217, 1EJG Pro36, 1US0 Glu64 and Lys307). The 166 clearly interpretable single-residue examples with verified C β shifts $\geq 0.2\text{\AA}$ were then classified as exhibiting either backrub movement (as described below) or some other type of movement.

Definition of backrub movement and BACKRUB modeling: A backrub motion shifts the position of the C α -C β bond vector for residue i by a backbone change that is low energy (i.e., maintains essentially ideal bond lengths, bond angles, and peptide planarity) and is purely local (i.e., with essentially no motion of C $\alpha_{i\pm 1}$ and none at all beyond C $\alpha_{i\pm 2}$). The BACKRUB modeling algorithm, described below, closely satisfies the backrub paradigm using 3 rotations around C α -C α axes. Successful modeling of a putative backrub motion using the BACKRUB software means that all clearly visible sidechain and backbone atom positions in both conformations can be well fit by two states of a single, closely-ideal model which differ only by adjustment of the 3 variable BACKRUB parameters, plus χ angles for sidechain i .

BACKRUB algorithm for software tools: A preliminary exploration of backrub motions was done by a brute-force sampling of ϕ, ψ, τ space that built model halves separately inward from C α_{i-1} and C α_{i+1} to meet at a resulting C α_i within 0.02Å, disallowing Ramachandran outliers and limiting non-ideality of τ (Figure 1). This search produces a fan of permissible conformations that swing the central C α -C β vector perpendicular to the chain direction, as anticipated, with essentially no C β motion in other directions. However, the ϕ, ψ plots of Figure 1 show that the relationships are non-linear and complex. The curve shapes differ for different starting conformations and for residue $i-1$ versus $i+1$, and they show much more spread with variation of $\tau_{i\pm 1}$ in the β

than in the α region. (Banding is an artifact of a 3° sampling interval in τ .) Interestingly, ϕ and ψ change very little for the central residue i whose sidechain is moving. These complex relationships prevented derivation of an analytical expression for this motion.

The simplified BACKRUB algorithm (Figure 2) was developed for practical use, with only three independent variables. It produces an extremely close approximation of a backrub motion by user control of rigid-body rotations around $C\alpha$ - $C\alpha$ vectors: a two-peptide rotation and two single-peptide rotations. The BACKRUB algorithm was implemented in Java as a tool in KiNG. Its use requires specifying the appropriate PDB-format coordinate file (with hydrogens) and activates a dialog box to control the rotations, with informational displays that warn of Ramachandran outliers (Lovell et al., 2003) or τ angles $> 1\sigma$ from ideal (Engh and Huber, 1991). The BACKRUB tool can be active at the same time as the sidechain-rotamer and rotation tool in KiNG, which is similar to the sidechain tool described for MAGE (Richardson et al., 2003; Word et al., 2000). The KiNG software and related programs are available, free and open-source, from <http://kinemage.biochem.duke.edu>.

The geometry used by the BACKRUB algorithm is diagrammed in Figure 2a. It acts on a central residue i and the two flanking peptides. For each of three different rotational components, a subgroup of atoms moves as a rigid body around some (virtual) axis. The primary component of motion rotates all atoms between the $C\alpha$'s of residue $i-1$ and $i+1$ around an axis between $C\alpha_{i-1}$ and $C\alpha_{i+1}$. This produces a wide arcing motion of the sidechain roughly perpendicular to the overall local chain direction. The two secondary components rotate the four central atoms of a peptide group around an axis between the $C\alpha$'s on either end, which helps alleviate τ -angle or H-bond strain introduced by the primary motion. All bond lengths and angles are invariant except for the three τ angles. In Figure 2b the substates differ only by the primary rotation, while in 2c the peptides have been rotated to help preserve the H-bonding CO and NH positions.

The BACKRUB algorithm closely approximates the common backrub mode of local backbone plasticity (see Discussion). However, it should be noted that there are many other changes in backbone conformation to which it is not applicable. Its area of effect is deliberately small, and so it is not suited for motions of large chain segments. Since it assumes fixed anchor points at either end, it cannot be used for domain hinges or immediately next to chain ends. A generalization of BACKRUB to act between arbitrary $C\alpha$'s was explored, but it introduces further complications while adding only a few additional successes at fitting changes in longer loops.

To aid in the assignment of backrub motion vs. other motion for each alternate conformation example, modeling of changes was tested using the BACKRUB tool in KiNG for more than half of the 166 cases, including all large or complex motions and multiple examples of each recognizable pattern of change (e.g., serines similar to Fig. 3b). If backbone atoms had been assigned alternate positions in the PDB file, then the conformation with more ideal peptide geometry (usually A) was taken as the starting point for modeling the second (B) alternate conformation, using only the three BACKRUB rotations and the sidechain χ dihedrals with idealized sidechain geometry, and

emphasizing fit to the atoms most clearly observed in the electron density. In some cases, both original conformations had substantial but opposite distortions in covalent geometry; a more nearly ideal intermediate would make a better BACKRUB starting point, but we very seldom added such a step (e.g. Kin. 6 in the supplement). Criteria of good fit were the same as would be applied in crystallographic rebuilding at this resolution. If alternates had been assigned starting only at C β , then the common backbone conformation was taken as the starting point, with an idealized C β (Lovell et al., 2003) (usually halfway between the two assigned C β positions) and ideal-geometry sidechain (Engh and Huber, 1991); then both A and B conformations were modeled using BACKRUB motions in opposite directions. These BACKRUB models are shown in orange in the figures, where their fit to deposited models and to electron density can be judged.

For correction of an experimental model misfit into the wrong local-minimum conformation during crystallographic refinement (e.g., Figure 4), first the new sidechain rotamer was chosen, next the backbone was shifted with the BACKRUB tool, and finally both backbone and sidechain rotations were adjusted to optimize all-atom contacts and electron density fit.

Results

We first present a survey of backbone plasticity as revealed by the alternate conformations in a set of sub-1Å x-ray crystallographic structures totaling nearly 4000 residues. These data show that backrub motions are quite common, and that the BACKRUB algorithm is sufficient to create realistic models that closely match the experimental observations. We then illustrate the process of using BACKRUB for refitting during the structure determination process. A table of examples, 3D kinemage graphics, selected coordinates, and a README file are available as supplementary material.

The 19 structures surveyed are described in Table 1. Of alternate conformations that shift backbone for a dipeptide or less, 76% are backrub motions (126/166, listed in the Supplement). Globally, then, 3.2% (126/3882) of all the residues in these structures are well modeled as a backrub change in backbone conformation. This is a conservative estimate, omitting examples that can be modeled successfully without C β shift (e.g. 1N9B Leu30), but not considering the complementary cases best modeled as significant C β shifts but not deposited as such (e.g. 1PQ7 Cys57). Serine is far the most common amino acid seen, making up 25% of backrubs. Two factors could explain their predominance: Ser is the smallest rotatable sidechain, and it has many choices of donor or acceptor H-bond partners, some of which are local enough to constrain these slight backbone shifts. Most alternate conformations of any type occur at the protein surface, and polar sidechains predominate; Lys, Arg, and Glu contribute 8% of backrubs each. Of the hydrophobics, Val, Met, and Leu occur most often.

Other types of backbone motions observed include peptide flips (a 3-peptide change in which the central peptide rotates by 90-180°), usually in tight turns. They can be identified even within long stretches of concerted motion, but are still much rarer than backrubs, with only 4 cases in this dataset: 1GWE 105, 1IX9 135, 1MUW 174, 1US0 93.

Intermediate rotations of single peptides are identifiable from large displacements of the carbonyl O density: many can be fit well with the BACKRUB tool (e.g. 1PQ7 Ser132, 1US0 Arg40) although the sidechain does not always move (e.g. 1N9B Ser41, which preserves two helix N-cap H-bonds through waters; coordinates in the supplement). The single-residue “other” cases include four large movements of chain-terminal residues, which are unconstrained on one side and thus have very different properties.

Figure 3a and b compare two different relationships seen for alternate-conformation serines, the most frequent backrub amino acid. These and other examples are available as animated, 3D kinemage graphics in the Supplement. Figure 3a shows Ser34 in an $\alpha\beta$ loop of the 1N9B TIM barrel, with a large C β shift of 1.02Å. Alternates were defined for all atoms in residue 34 but not the rest of the two peptides. This represents the changes reasonably well but gives highly non-planar peptides for which there is no direct evidence; a pair of BACKRUB models fits the density equally well with nearly ideal geometry. Electron density for the carbonyl oxygen is highly anisotropic, indicating a single-peptide rotation that reinforces the primary backrub rotation rather than the usual compensation that preserves backbone H-bonding (Fig. 2c). Ser34 alternate conformations are coupled to those of Arg250 (not shown), making or breaking an H-bond to the Ser O γ . The Ser sidechain moves but does not change rotamer conformation; this is unusual, since 108 out of 126 backrub cases (86%) show distinct sidechain rotamers, as is also true for most single-residue “other” cases. 87 of the backrubs with distinct rotamers have χ_1 in distinct local minima, as in Fig. 3b and d. Backbone alternates without a rotamer change usually show distinct H-bond states for either sidechain (Fig 3a) or backbone.

Figure 3b shows 1DY5 SerA15, a more typical serine backrub example with distinct rotamers and H-bonds from a clear 0.46Å C β shift, implying a backbone movement. Alternates were defined in the PDB file for C β but not for any backbone atoms (*white*), producing bond-angle distortions up to 9° around C α and C β . Here also, a pair of BACKRUB models (*orange*) fits the electron density equally well with τ deviations under 1 σ (3°) and completely ideal geometry otherwise. The asymmetrical T shape of the sidechain electron density for SerA15 is the usual pattern for serines with C β alternates (e.g. 1MUW Ser69, 1DY5 SerB50 in supplement). One conformation (here, with O γ pointing left) has no strong positive or negative constraints, its rotamer is excellent, and its backbone conformation is presumably relaxed. The second conformation makes a favorable but constrained H-bond (to a backbone CO) which is not accessible with a good rotamer and good geometry from the other C β position. Thus, the C β is pushed back significantly (causing a backrub shift) and the sidechain finds a compromise between H-bond strength and favorable χ_1 angle. The Ser15 backbone CO stays in position and H-bonded. Ser15 in chain B shows the same pattern, which is usually but not always the case between subunit pairs with non-crystallographic symmetry.

Lys100 from 1US0 displays even clearer and more extensive alternate-conformation electron density (Fig. 3c), with 3 σ peaks (*purple*) for all sidechain atoms in each conformation, including the C β s 0.97Å apart. Strong anisotropy of backbone density

indicates motion of those atoms also. Lys100 combines backbone and sidechain motion to leave N ζ in place (top right in Fig. 3c), maintaining two H-bonds to backbone carbonyls and a weaker interaction with Asn52 O δ . The B alternate is a good rotamer (*mtmm*) (Lovell et al., 2000) and the A alternate an acceptable one (*mppt*). Lys100 forms the C-cap of an α helix (Richardson and Richardson, 1988), and its backbone H-bonds are apparently preserved by a concerted smaller backrub motion of Ser97. Backrub motions are less common and smaller within helices, where steric constraints from neighboring turns limit the magnitude of motion in the backrub direction. They are most common in β strands or extended loops. Another case of concerted backrub motion between two interacting residues is Tyr378 of 1GWE (see Supplement), one conformer of which would intersect its 2-fold equivalent in another subunit if both were occupied simultaneously.

Fig. 3d shows Ile47 of 1N9B. Well-separated electron density peaks for all 6 C γ and C δ atoms in the two distinct sidechain rotamers unambiguously mandate two C β positions and two backbone conformations, which are fit by the two BACKRUB models (*orange/peach*) with near-ideal geometry for both backbone and sidechain. This is a prototypical case in which the two peptides counter-rotate somewhat against the primary BACKRUB rotation and preserve all 4 β -sheet H-bonds (lenses of green contact dots, with both conformations overlaid in the figure). Another example of sidechain motion with backrub-maintained β sheet is Thr268 of 1R6J.

In this analysis, several amino acid types are special cases. Glycine was ruled out by definition, since it has no C β to show a shift. Only one alanine is represented (1N9B Ala257), presumably because Ala sidechains have neither rotamer nor H-bond states to drive local backbone shifts. Cysteine alternates are frequently driven by breaking the disulfide; rotamers may or may not change (1PQ7 Cys41 in Supplement, 1N9B Cys123). Cys or Met alternates can often be analyzed at somewhat lower resolutions, if the heavy S atoms are clearly visible. Eight prolines have C β alternates fit $>0.2\text{\AA}$ apart, one alternate in each ring pucker (C γ endo and C γ exo). Half of them can be fit well by BACKRUB, including the skewed relationship of C γ positions, but it is unclear whether that is the best description. Analysis of proline alternates is hampered by overlapping density for most atoms and by errors (Engh and Huber, 2002) in geometry values currently used for proline (Engh and Huber, 1991), which would cause some bias even at these high resolutions. Arginine displays especially varied and elegant patterns of alternate conformations because of guanidinium size and H-bonding (e.g. 1SSX Arg120, 192; 1MUW Arg204).

Figure 4 shows an example of using the BACKRUB software tool for model rebuilding during crystallographic refinement: IleA120 from 1MO0. In addition to representing real backbone plasticity as shown above, BACKRUB is also very effective for rebuilding because it moves one C α and the neighboring peptides by a small amount, but dramatically alters the accessible rotamers by swinging the whole sidechain on a long lever arm. In the original conformation of Fig. 4a, all-atom contacts (Word et al., 2000; Word et al., 1999a) indicate severe steric clashes with surrounding atoms, and difference

peaks in the F_o-F_c map suggest that χ_1 is off by 120° . When the correct sidechain rotamer is fit on the original backbone (Fig. 4b), the serious steric clashes are all on one side, with space on the other side. A BACKRUB movement swings the sidechain to establish excellent packing interactions all around (Fig. 4c). Additional evidence strongly supports the correction: sidechain rotamericities improve, difference density is satisfied, and the new model matches Ile120 of chain B. Final confirmation comes from improved re-refinement (Arendall et al., 2005).

Discussion

The alternate conformations seen in sub-1Å-resolution crystal structures show unambiguously that protein backbone often exhibits highly localized, small-amplitude plasticity that is tightly coupled to larger, 2-state conformational change of the sidechain. By far the commonest case is a “backrub” motion, in which one residue and its adjacent peptides twist slightly around the backbone; this is usually driven by a change in sidechain rotamer and/or hydrogen bonding partners, leading to significant sidechain motion perpendicular to the chain direction. Over the 19 proteins and 3882 residues studied here, 1 residue in 30 clearly shows a backrub motion (126 examples), and backrub motions are surely even more prevalent under physiological or solution conditions than in frozen crystals.

The BACKRUB algorithm described here produces geometrically and sterically reasonable models that fit the electron density extremely well. Its utility in crystallographic rebuilding is demonstrated in Figure 4 (see above) and in Arendall et al. (2005). In practice, BACKRUB is most useful either for defining alternate conformations at very high resolution or for correctional rebuilding of backbone in the 2 to 3Å resolution range. At resolutions $<2\text{Å}$, backbone atom positions are strongly constrained, so a sidechain misfit into the wrong rotamer produces distorted bond angles instead (Lovell et al., 2003). At resolutions $>3\text{Å}$, one cannot address such fine detail, due to surrounding inaccuracies.

Backrub motion is large for the central sidechain, moderate for its backbone, and decreases rapidly on either side. To accomplish a “true” low-energy backrub movement with essentially pure ϕ, ψ variables, as proteins presumably do, extremely small changes would propagate past the $i\pm 1$ $C\alpha$ atoms. This involves at least five pairs of ϕ, ψ angle changes and an intractable level of complexity. As the figures show, however, BACKRUB-generated models are remarkably good at fitting the electron density of alternate conformations with only three variables besides sidechain rotamer. Sidechain rotamers (Lovell et al., 2000) are essentially always favorable, and all bond lengths, bond angles, and peptide planarity can be kept ideal except for the τ bond angles at $C\alpha$ $i-1$, i , and $i+1$. Those τ distortions seldom exceed one standard deviation (Engh and Huber, 1991), and sometimes ideality is improved. Of course, any BACKRUB refitting during solution of a crystal structure would be submitted to further refinement afterward. A small percentage of cases appear to require non-ideal rotamers or geometry (especially buried Met or disulfides) and may actually have both conformations strained by the tight surroundings

rather than both favorable. Different approximate fitting procedures that are commonly used for crystallography include allowing a sidechain to shift independently of the backbone or allowing one residue to shift independently of its neighbors. Those techniques are not significantly simpler than the BACKRUB, but they produce very large distortions of bond angles or peptide planarity not supported by the data.

It seems likely that other modes of local backbone plasticity remain to be discovered. This is particularly true of α -helices, where backrub motions are less common than in extended structure. Some examples of helix motions combine winding and unwinding to shift a local region sideways without disrupting the overall helix (e.g. 1EJG 6-9), but no other local helix modes were common enough for classification. Peptide flips were observed in loops, but only rarely.

On the evolutionary time scale, local backrub shifts could be an important component of protein robustness to point mutations, accommodating sidechains of different sizes and shapes without radically altering the backbone scaffold. However, it is difficult to observe backrub motions directly by comparing structures of point mutants because the coordinate error between two “identical” but independently refined structures is a few tenths of an Ångstrom, comparable to the size of the backrub conformational changes (DePristo et al., 2003; Kleywegt, 1999). Thus, we turned instead to the more accurate and quite numerous examples of backrub motion found within single crystal structures. The magnitude of such backbone movement is small: 90% of the examples shift $C\beta < 0.8\text{Å}$, and 50% by $< 0.4\text{Å}$, while $C\alpha$ and other backbone atoms move half that much or less. However, essentially all cases leverage sidechain atom shifts of 1 to 8Å (2.8Å on average), quite like the change necessitated by a sequence difference. Nearly all local backbone motions in alternate conformations are coupled to sidechain switches between rotamers (86%), which have steric and electrostatic consequences on par with the effects of a point mutation. Thus, we believe alternate conformations provide a good model of how a backrub motion could be involved in preserving a protein’s structure as its sequence evolves. Of even more immediate practical relevance, the backrub motion should provide a conservative backbone “move”, of well documented occurrence in accurate experimental structures, to help protein design and homology modeling calculations provide the local backbone adjustments required for successful accommodation of sequence changes.

These observations are also directly relevant to protein dynamics, in spite of their origin in data from highly ordered crystals at cryogenic temperatures. Individual crystal structures are not usually thought of as dynamic, both because crystallization selects only a subset of the conformations populated in solution, and also because at most accessible resolutions alternate conformations are manifested only by lowered electron density and are thus seldom modeled in the coordinates. At very high resolution, however, multiple conformations become directly visible (2 or occasionally 3 copies, down to perhaps 10% occupancy in the best cases). At the cryogenic temperatures typical of modern data collection (near 100 K) presumably no large dynamic fluctuations occur in individual molecules, so alternate conformations represent static disorder between molecules, a

sample of the conformations present in the room-temperature crystal. In the other direction, however, it is quite certain that the conformations seen in these structures are also present in solution—thus they show the geometry of a valid subset of protein motions.

Crystallographic alternate conformations imply that the states must have comparable energies, since their observable fractional occurrences lie between 1:1 and at most 10:1. (an energy difference of kT yields a 3:1 ratio). For these $C\beta$ -shift cases that imply backbone motion, the mobile sidechain atoms nearly always show clearly separated peaks, implying an energy barrier between the sidechain states. The backbone atoms, in contrast, nearly always show continuous density between positions close in space, implying that the backbone stays within a single local energy well. As shown above, backrub motions also have the important ability to preserve NH and CO orientations that control backbone H-bonds, thus preserving secondary structure despite substantial sidechain movement. This set of properties is here only shown to hold for the low-energy subset of motions manifested in high-resolution crystal structures, but it matches well with the properties seen by NMR order parameters and other dynamical measurements: relatively less motion of the highly H-bonded peptide NH's than for the carbonyl- $C\alpha$ bonds (Wang et al., 2003), and greater and more complex motion for the sidechains (Kay, 2005; Palmer, 2004), most of which visit multiple separate rotamer states (Chou et al., 2003). As a detailed description of a common, experimentally verified local movement, backrub fluctuations provide a new model—in addition to out-of-plane amide vibrations (Palmo et al., 2003) or crankshaft peptide motions (Fadel et al., 1995)—for the analysis of NH order parameters, with the valuable feature of built-in coupling to larger sidechain motions.

Spectroscopic methods dominate the experimental study of protein dynamics because they can measure time scales, relative magnitudes, and even energetics of motions. However, any inference about the pattern of movement in space is highly indirect. In contrast, high-resolution crystal structures can give no insight into time scales, but they show a direct image of what atoms are moving where, and they constitute a valuable and largely untapped source of dynamic information. Here we have used crystallographic alternate conformations to demonstrate a form of local backbone plasticity that appears to dominate small-scale accommodation to sidechain rotamer fluctuations and perhaps also to single-site mutations. These results also strongly imply that backbone and sidechain dynamics should not be analyzed in isolation, since for at least one common mode the two are tightly coupled.

Acknowledgements

We thank Wolfram Tempel and B.C. Wang for SECSG collaboration on using the BACKRUB tool in structure improvement, Jack Snoeyink for collaboration on inverse kinematics of protein backbone, Gerard Kleywegt for providing F_o-F_c as well as $2F_o-F_c$ maps on the Electron Density Server site, and the crystallographers who deposited these

high-resolution structures and data. Support was from NIH GM-15000, GM-073930, P50 GM-62407, and a HHMI Predoctoral Fellowship to IWD.

References

- Addlagatta, A., Krzywda, S., Czapinska, H., Otlewski, J., and Jaskolski, M. (2001). Ultrahigh-resolution structure of a BPTI mutant. *Acta Crystallogr D Biol Crystallogr* 57, 649-663.
- Arendall, W. B., Tempel, W., Richardson, J. S., Zhou, W., Wang, S., Davis, I. W., Liu, Z. J., Rose, J. P., Carson, M., Luo, M., *et al.* (2005). A Test Of Enhancing Model Accuracy In High-Throughput Crystallography. *The Journal of Structural and Functional Genomics* 6, 1-11.
- Bahar, I., Erman, B., Haliloglu, T., and Jernigan, R. L. (1997). Efficient characterization of collective motions and interresidue correlations in proteins by low-resolution simulations. *Biochemistry* 36, 13512-13523.
- Baldwin, E. P., Hajiseyedjavadi, O., Baase, W. A., and Matthews, B. W. (1993). The Role of Backbone Flexibility in the Accommodation of Variants That Repack the Core of T4 Lysozyme. *Science* 262, 1715-1718.
- Berman, H. M., Westbrook, J., Feng, Z., Gilliland, G., Bhat, T. N., Weissig, H., Shindyalov, I. N., and Bourne, P. E. (2000). The Protein Data Bank. *Nucleic Acids Research* 28, 235-242.
- Blaszczyk, J., Li, Y., Shi, G., Yan, H., and Ji, X. (2003). Dynamic roles of arginine residues 82 and 92 of Escherichia coli 6-hydroxymethyl-7,8-dihydropterin pyrophosphokinase: crystallographic studies. *Biochemistry* 42, 1573-1580.
- Cavanagh, J., Fairbrother, W. J., Palmer, I., A.G., and Skelton, N. J. (1996). *Protein NMR Spectroscopy: Principles and Practice* (San Diego, Academic Press).
- Chou, J. J., Case, D. A., and Bax, A. (2003). Insights into the mobility of methyl-bearing side chains in proteins from $(3)J(CC)$ and $(3)J(CN)$ couplings. *J Am Chem Soc* 125, 8959-8966.
- Dahiyat, B. I., and Mayo, S. L. (1997). *De Novo* Protein Design: Fully Automated Sequence Selection. *Science* 278, 82-87.
- Davis, I. W., Murray, L. W., Richardson, J. S., and Richardson, D. C. (2004). MOLPROBITY: structure validation and all-atom contact analysis for nucleic acids and their complexes. *Nucleic Acids Res* 32, W615-619.
- DePristo, M. A., de Bakker, P. I., Lovell, S. C., and Blundell, T. L. (2003). Ab initio construction of polypeptide fragments: efficient generation of accurate, representative ensembles. *Proteins* 51, 41-55.
- Desjarlais, J. R., and Handel, T. M. (1995). *De novo* design of the hydrophobic cores of proteins. *Protein Science* 4, 2006-2018.
- Engh, R. A., and Huber, R. (1991). Accurate Bond and Angle Parameters for X-ray Protein Structure Refinement. *Acta Crystallographica, Section A* 47, 392-400.
- Engh, R. A., and Huber, R. (2002). Structure quality and target parameters. In *International Tables for Crystallography F*, M. G. Rossman, and E. Arnold, eds.
- Erskine, P. T., Coates, L., Mall, S., Gill, R. S., Wood, S. P., Myles, D. A., and Cooper, J. B. (2003). Atomic resolution analysis of the catalytic site of an aspartic proteinase and an unexpected mode of binding by short peptides. *Protein Science* 12, 1741-1749.

Esposito, L., Vitagliano, L., Sica, F., Sorrentino, G., Zagari, A., and Mazzarella, L. (2000). The ultrahigh resolution crystal structure of ribonuclease A containing an isoaspartyl residue: hydration and stereochemical analysis. *J Mol Biol* 297, 713-732.

Fadel, A. R., Jin, D. Q., Montelione, G. T., and Levy, R. M. (1995). Crankshaft motions of the polypeptide backbone in molecular dynamics simulations of human type-alpha transforming growth factor. *J Biomol NMR* 6, 221-226.

Fenn, T. D., Ringe, D., and Petsko, G. A. (2004). Xylose isomerase in substrate and inhibitor michaelis states: atomic resolution studies of a metal-mediated hydride shift. *Biochemistry* 43, 6464-6474.

Fuhrmann, C. N., Kelch, B. A., Ota, N., and Agard, D. A. (2004). The 0.83 Å resolution crystal structure of alpha-lytic protease reveals the detailed structure of the active site and identifies a source of conformational strain. *J Mol Biol* 338, 999-1013.

Gassner, N. C., Baase, W. A., and Matthews, B. W. (1996). A test of the "jigsaw puzzle" model for protein folding by multiple methionine substitutions within the core of T4 lysozyme. *Proceedings of the National Academy of Sciences of the United States of America* 93, 12155-12158.

Getzoff, E. D., Gutwin, K. N., and Genick, U. K. (2003). Anticipatory active-site motions and chromophore distortion prime photoreceptor PYP for light activation. *Nat Struct Biol* 10, 663-668.

Howard, E. I., Sanishvili, R., Cachau, R. E., Mitschler, A., Chevrier, B., Barth, P., Lamour, V., Van Zandt, M., Sibley, E., Bon, C., *et al.* (2004). Ultrahigh resolution drug design I: details of interactions in human aldose reductase-inhibitor complex at 0.66 Å. *Proteins* 55, 792-804.

Hu, H., Elstner, M., and Hermans, J. (2003). Comparison of a QM/MM force field and molecular mechanics force fields in simulations of alanine and glycine "dipeptides" (Ace-Ala-Nme and Ace-Gly-Nme) in water in relation to the problem of modeling the unfolded peptide backbone in solution. *Proteins: Structure, Function and Genetics* 50, 451-463.

Jelsch, C., Teeter, M. M., Lamzin, V., Pichon-Lesme, V., Blessing, R. H., and Lecomte, C. (2000). Accurate Protein Crystallography at Ultra-High Resolution: Valence-Electron Distribution in Crambin. *Proceedings of the National Academy of Sciences of the United States of America* 97, 3171-3176.

Kang, B. S., Devedjiev, Y., Derewenda, U., and Derewenda, Z. S. (2004). The PDZ2 domain of syntenin at ultra-high resolution: bridging the gap between macromolecular and small molecule crystallography. *J Mol Biol* 338, 483-493.

Karplus, M., and McCammon, J. A. (2002). Molecular dynamics simulations of biomolecules. *Nat Struct Biol* 9, 646-652.

Kay, L. E. (2005). NMR studies of protein structure and dynamics. *J Magn Reson* 173, 193-207.

Kleywegt, G. J. (1999). Experimental assessment of differences between related protein crystal structures. *Acta Crystallographica Section D* 55, 1878-1884.

Kleywegt, G. J., Harris, M. R., Zou, J. Y., Taylor, T. C., Wahlby, A., and Jones, T. A. (2004). The Uppsala Electron-Density Server. *Acta Crystallogr D Biol Crystallogr* 60, 2240-2249.

Ko, T. P., Robinson, H., Gao, Y. G., Cheng, C. H., DeVries, A. L., and Wang, A. H. (2003). The refined crystal structure of an eel pout type III antifreeze protein RD1 at 0.62-Å resolution reveals structural microheterogeneity of protein and solvation. *Biophys J* 84, 1228-1237.

Kursula, I., and Wierenga, R. K. (2003). Crystal structure of triosephosphate isomerase complexed with 2-phosphoglycolate at 0.83-Å resolution. *J Biol Chem* 278, 9544-9551.

Lim, W. A., and Sauer, R. T. (1989). Alternative packing arrangements in the hydrophobic core of λ repressor. *Nature* 339, 31-36.

Lipari, G., Szabo, A., and Levy, R. M. (1982). Protein dynamics and NMR relaxation: comparison of simulations with experiment. *Nature* 300, 197-198.

Liu, L., Nogi, T., Kobayashi, M., Nozawa, T., and Miki, K. (2002). Ultrahigh-resolution structure of high-potential iron-sulfur protein from *Thermochromatium tepidum*. *Acta Crystallogr D Biol Crystallogr* 58, 1085-1091.

Liu, Q., Huang, Q., Teng, M., Weeks, C. M., Jelsch, C., Zhang, R., and Niu, L. (2003). The crystal structure of a novel, inactive, lysine 49 PLA2 from *Agkistrodon acutus* venom: an ultrahigh resolution, AB initio structure determination. *J Biol Chem* 278, 41400-41408.

Looger, L. L., Dwyer, M. A., Smith, J. J., and Hellinga, H. W. (2003). Computational design of receptor and sensor proteins with novel functions. *Nature* 423, 185-190.

Lovell, S. C., Davis, I. W., Arendall, W. B., III, Bakker, P. I. W. d., Word, J. M., Prisant, M. G., Richardson, J. S., and Richardson, D. C. (2003). Structure Validation by C α Geometry: ϕ, ψ and C β Deviation. *Proteins: Structure, Function and Genetics* 50, 437-450.

Lovell, S. C., Word, J. M., Richardson, J. S., and Richardson, D. C. (2000). The penultimate rotamer library. *Proteins: Structure, Function, and Genetics* 40, 389-408.

Matthews, B. W. (1995). Studies on protein stability with T4 lysozyme. *Advances in Protein Chemistry* 46, 249-278.

Mooers, B. H., Datta, D., Baase, W. A., Zollars, E. S., Mayo, S. L., and Matthews, B. W. (2003). Repacking the Core of T4 lysozyme by automated design. *Journal of Molecular Biology* 332, 741-756.

Munson, M., O'Brien, R., Sturtevant, J. M., and Regan, L. (1994). Redesigning the hydrophobic core of a four-helix-bundle protein. *Protein Science* 3, 2015-2022.

Murshudov, G. N., Grebenko, A. I., Brannigan, J. A., Antson, A. A., Barynin, V. V., Dodson, G. G., Dauter, Z., Wilson, K. S., and Melik-Adamyanyan, W. R. (2002). The structures of *Micrococcus lysodeikticus* catalase, its ferryl intermediate (compound II) and NADPH complex. *Acta Crystallogr D Biol Crystallogr* 58, 1972-1982.

Noonan, K., O'Brien, D., and Snoeyink, J. (2004). Probik: Protein Backbone Motion by Inverse Kinematics. Paper presented at: Workshop on the Algorithmic Foundations of Robotics (Springer Verlag).

Nukaga, M., Mayama, K., Hujer, A. M., Bonomo, R. A., and Knox, J. R. (2003). Ultrahigh resolution structure of a class A beta-lactamase: on the mechanism and specificity of the extended-spectrum SHV-2 enzyme. *J Mol Biol* 328, 289-301.

Palmer, I., A.G. (2004). NMR characterization of the dynamics of biomacromolecules. *Chem Rev* 104, 3623-3640.

Palmo, K., Mannfors, B., Mirkin, N. G., and Krimm, S. (2003). Potential energy functions: from consistent force fields to spectroscopically determined polarizable force fields. *Biopolymers* 68, 383-394.

Patterson, W. R., Anderson, D. H., DeGrado, W. F., Cascio, D., and Eisenberg, D. (1999). Centrosymmetric bilayers in the 0.75 Å resolution structure of a designed alpha-helical peptide, D,L-Alpha-1. *Protein Science* 8, 1410-1422.

Qian, B., Ortiz, A. R., and Baker, D. (2004). Improvement of comparative model accuracy by free-energy optimization along principal components of natural structural variation. *Proc Natl Acad Sci U S A* 101, 15346-15351.

Richardson, J. S., Arendall, W. B., III, and Richardson, D. C. (2003). New Tools and Data for Improving Structures, Using All-atom Contacts. In *Methods in Enzymology*, vol. 374, C. W. Carter, Jr., and R. M. Sweet, eds. (New York, Academic Press), pp. 385-412.

Richardson, J. S., and Richardson, D. C. (1988). Amino Acid Preferences for Specific Locations at the Ends of α -Helices. *Science* 240, 1648-1652.

Richardson, J. S., Richardson, D. C., Tweedy, N. B., Gernert, K. M., Quinn, T. P., Hecht, M. H., Erickson, B. W., Yan, Y., McClain, R. D., Donlan, M. E., and Surles, M. C. (1992). Looking at proteins: representations, folding, packing, and design. *Biophysical Journal* 63, 1186-1209.

Rohl, C. A., Strauss, C. E., Misura, K. M., and Baker, D. (2004). Protein structure prediction using Rosetta. *Methods Enzymol* 383, 66-93.

Schmidt, A., Jelsch, C., Ostergaard, P., Rypniewski, W., and Lamzin, V. S. (2003). Trypsin revisited: crystallography AT (SUB) atomic resolution and quantum chemistry revealing details of catalysis. *J Biol Chem* 278, 43357-43362.

Schneider, T. R., and Sheldrick, G. M. (2002). Substructure solution with SHELXD. *Acta Crystallogr D Biol Crystallogr* 58, 1772-1779.

Tramontano, A., and Morea, V. (2003). Assessment of homology-based predictions in CASP5. *Proteins* 53 Suppl 6, 352-368.

van den Bedem, H., Lotan, I., Latombe, J. C., and Deacon, A. M. (2005). Real-space protein-model completion: an inverse-kinematics approach. *Acta Crystallogr D Biol Crystallogr* 61, 2-13.

Wang, T., Cai, S., and Zuiderweg, E. R. (2003). Temperature dependence of anisotropic protein backbone dynamics. *JACS* 125, 8639-8643.

Word, J. M., Bateman, R. C., Jr., Presley, B. K., Lovell, S. C., and Richardson, D. C. (2000). Exploring Steric Constraints on Protein Mutations using Mage/Probe. *Protein Science* 9, 2251-2259.

Word, J. M., Lovell, S. C., LaBean, T. H., Taylor, H. C., Zalis, M. E., Presley, B. K., Richardson, J. S., and Richardson, D. C. (1999a). Visualizing and Quantifying Molecular Goodness-of-Fit: Small-Probe Contact Dots with Explicit Hydrogens. *JMB* 285, 1711-1733.

Word, J. M., Lovell, S. C., Richardson, J. S., and Richardson, D. C. (1999b). Asparagine and Glutamine: Using Hydrogen Atom Contacts in the Choice of Side-chain Amide Orientation. *JMB* 285, 1735-1747.

Wuthrich, K. (1986). *NMR of Proteins and Nucleic Acids* (New York, Wiley).

Figure and Table Captions

Table 1: The set of protein structures surveyed for alternate backbone conformations.

PDB code	Description	Ref	Resol. (Å)	Total res.	Alt res.	Single alts	C β >0.2Å	Classifiable alternates	Backrubs
1EJG	Crambin (valence electron density)	(Jelsch et al., 2000)	0.54	48	19	17	7	6	5
1UCS	Type III antifreeze protein RD1	(Ko et al., 2003)	0.62	64	6	6	0	0	0
1US0	Human aldose reductase, with NADP+ and inhibitor	(Howard et al., 2004)	0.66	314	79	45	18	16	10
1R6j	Syntenin PDZ2	(Kang et al., 2004)	0.73	82	21	12	3	2	2
3AL1	Designed peptide α 1, racemic PI-bar form	(Patterson et al., 1999)	0.75	24	11	11	7	7	6
1IUUA	<i>Thermochromatium tepidum</i> HiPIP	(Liu et al., 2002)	0.80	83	6	6	2	2	2
1PQ7	Trypsin at pH 5 in borax	(Schmidt et al., 2003)	0.80	224	15	12	7	7	5
1NWZ	Photoactive yellow protein	(Getzoff et al., 2003)	0.82	125	25	12	8	7	6
1N55	E65Q mutant of <i>Leishmania</i> triosephosphate isomerase, with 2-phosphoglycolate	(Kursula and Vierenga, 2003)	0.83	249	33	31	22	18	9
1SSX	α -lytic protease at pH 8	(Fuhrmann et al., 2004)	0.83	198	23	23	17	13	11
1MC2	K49 phospholipase A2 homologue	(Liu et al., 2003)	0.85	122	10	10	4	3	3
1G6X	Bovine pancreatic trypsin inhibitor with mutated loop	(Addlagatta et al., 2001)	0.86	58	12	12	2	2	2
1MUW	Xylose isomerase	(Fenn et al., 2004)	0.86	386	79	70	24	16	12
1DY5	Deamidated bovine pancreatic ribonuclease	(Esposito et al., 2000)	0.87	246	39	39	23	22	21
1GWE	<i>Micrococcus lysodeikticus</i> catalase	(Murshudov et al., 2002)	0.88	498	47	40	9	8	5
1F9Y	<i>E. coli</i> HPPK with MgAMPCPP and 6-hydroxymethylpterin	(Blaszczuk et al., 2003)	0.89	158	21	21	3	3	2
1IX9	<i>E. coli</i> Mn(III) superoxide dismutase mutant	a	0.90	410	41	34	18	15	11
1N9B	Extended-spectrum SHV-2 β -lactamase	(Nukaga et al., 2003)	0.90	265	53	51	19	14	11
1OEW	Native endothiapsin	(Erskine et al., 2003)	0.90	328	29	24	7	5	3
total				3882	569	476	200	166	126

Alt res: residues with one or more atoms in alternate conformations

Single alts: alternate conformations that encompass at most one residue plus its peptides

C β >0.2Å: single alternates with C β positions separated by at least 0.2Å in the deposited model

Classifiable alternates: alternates with verified C β >0.2Å and clear enough electron density to infer mode of backbone change reliably

Backrubs: classifiable alternates that displayed backrub motion instead of some other type of motion

a: PDB file 1IX9 has no published journal reference; the depositors are B.F. Anderson, R.A. Edwards, M.M. Whittaker, E.N. Baker, G.B. Jameson (2002).

Figure 1: ϕ, ψ values for the $i+1$ (*orange*) and $i-1$ (*purple*) residues of conformations generated by a brute-force search of ϕ, ψ, τ space with invariant $C\alpha_{i-1}$ and $C\alpha_{i+1}$ positions; starting from either ideal α -helix (below center) or ideal β -sheet (top left). The ϕ, ψ angles are plotted within the contours of the updated Ramachandran plot from Lovell et al. (Lovell et al., 2003); parallel streaks of points result from coarse sampling of τ . All four dihedrals display complex, nonlinear relationships that are highly dependent on the starting conformation.

Figure 1

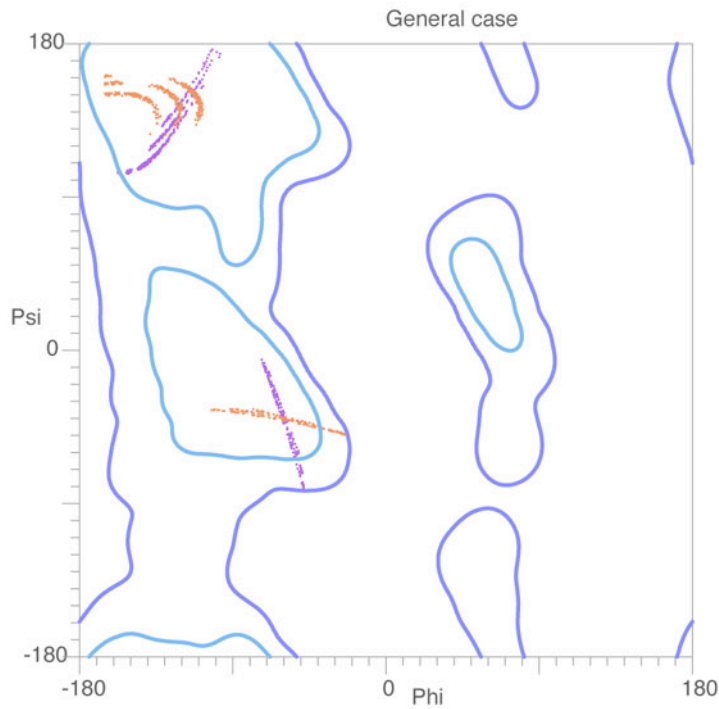


Figure 2: (a) A schematic diagram of the BACKRUB motion. The primary rotation ($\theta_{1,3}$) moves the central residue and its adjacent peptides around the red axis ($C\alpha^{i-1}$ to $C\alpha^{i+1}$) as a rigid body, causing the central $C\alpha$ to trace out the dotted circle. Secondary rotations ($\theta_{1,2}$ and $\theta_{2,3}$) move the individual peptides as rigid bodies around the blue $C\alpha$ - $C\alpha$ axes. A small amount of distortion is introduced into the τ angles (N- $C\alpha$ -C), but they generally remain well within the range of values seen in typical crystal structures. (b) A series of backbones generated with BACKRUB by making 5° steps around the primary rotation axis (hydrogens not shown). (c) Another series of backbones generated with BACKRUB by making 5° steps around the primary rotation axis, while also rotating each peptide to roughly maintain the H-bonding position of the NH and CO groups.

Figure 2

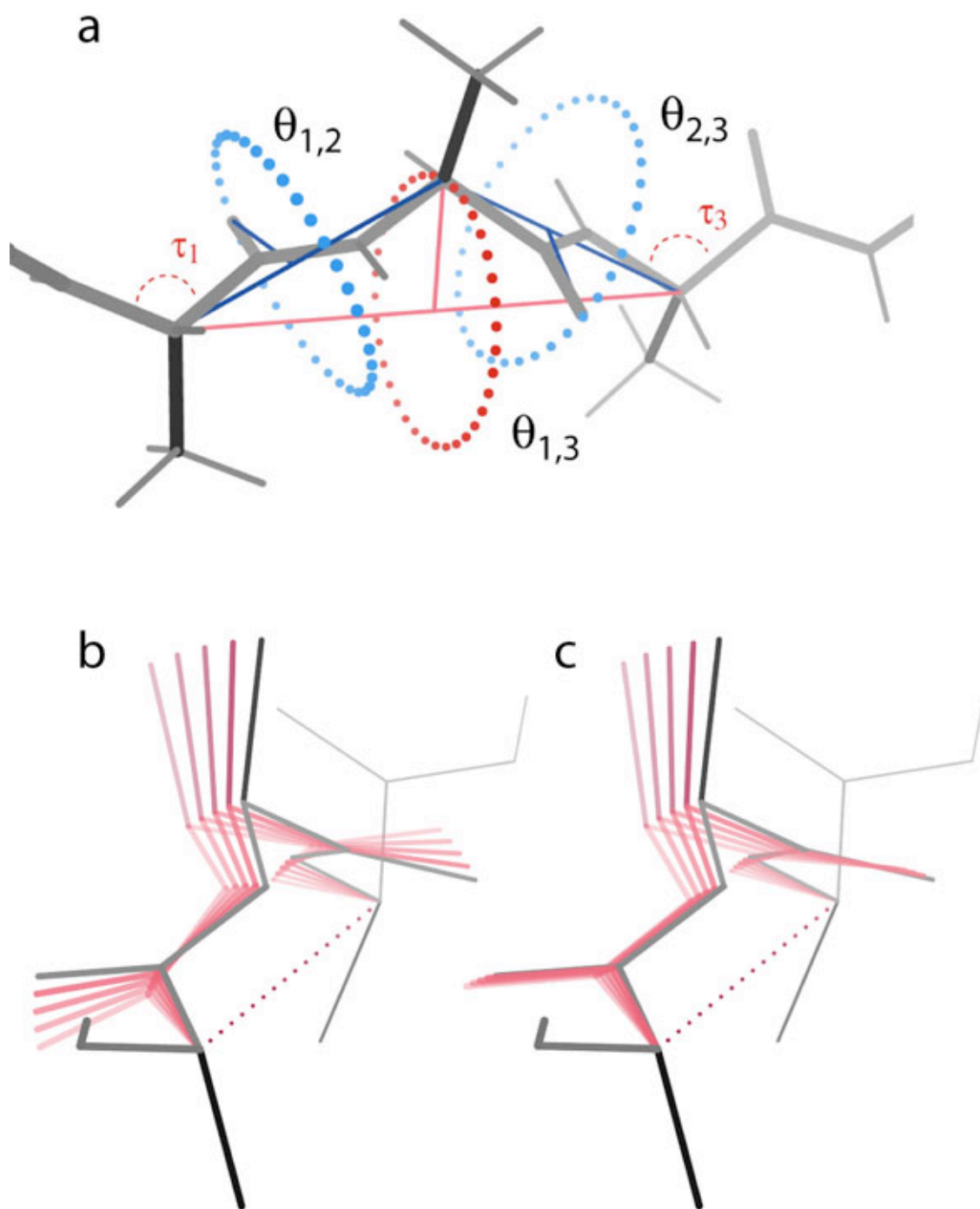


Figure 3: Examples of backrub motions observed in the alternate conformations of atomic-resolution crystal structures for two serines (the most commonly occurring backrub residue), a lysine, and an isoleucine. Original models are in white and cyan; BACKRUB-fit models are in orange. $2F_o-F_c$ maps contoured at 1.2σ are shown in gray; hydrogens are shown only in part b. See text for further details. (a) Ser 34 from 1N55. This residue moves in concert with Arg 250 to make/break an H-bond, but does not change rotamer. (b) Ser A15 from 1DY5, which changes both rotamer (χ_1 *m* vs. *p*) and H-bonding state to nearby backbone and to waters. (c) Lys 100 from 1US0, with rotamers *mppt* and *mtmm* both ending at the same H-bonded $N\zeta$ position. All alternate sidechain atoms show clearly separated density peaks at 3σ (*purple contours*). (d) Ile 47 from 1N9B, in rotamers *tt* and *mm*. BACKRUB models were fit for both A and B alternate conformations (*peach/orange*). The deposited model (not shown here) was fit without backbone alternates but had a $C\beta$ shift of 0.6\AA and the same two sidechain conformations as shown.

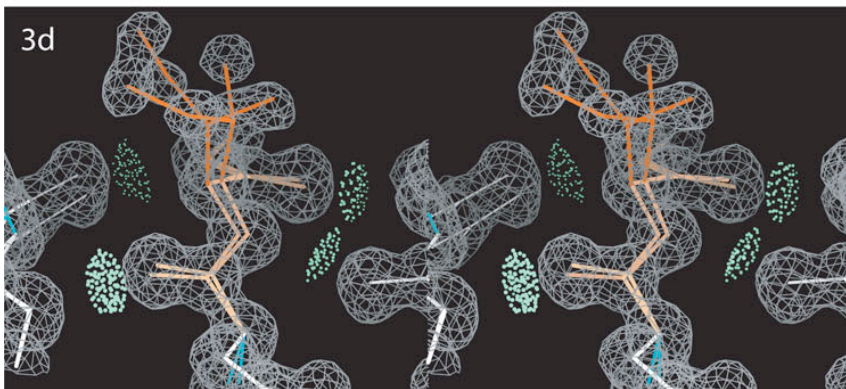
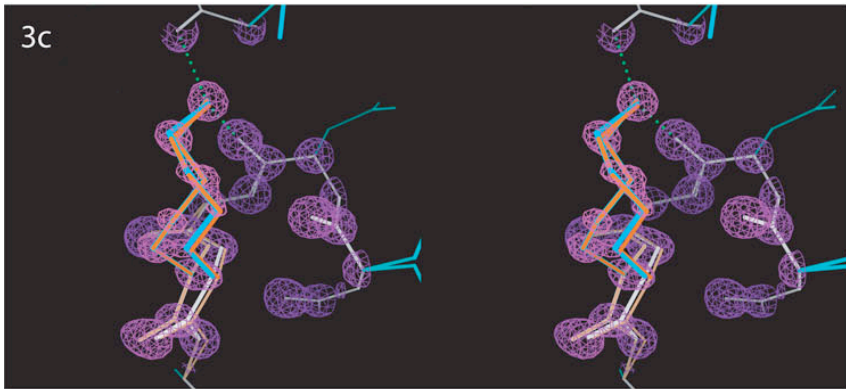
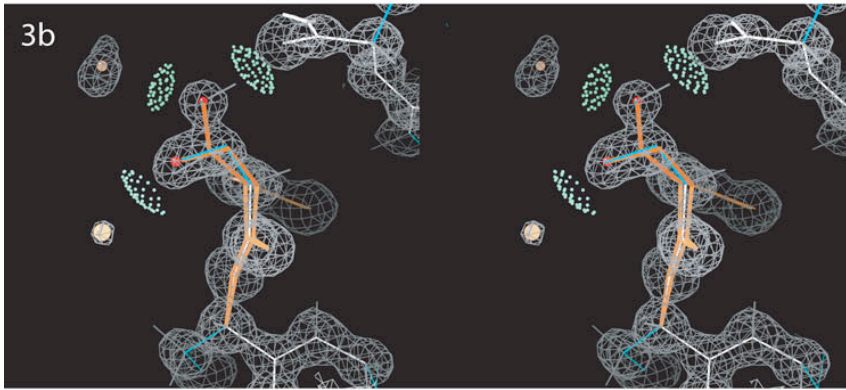
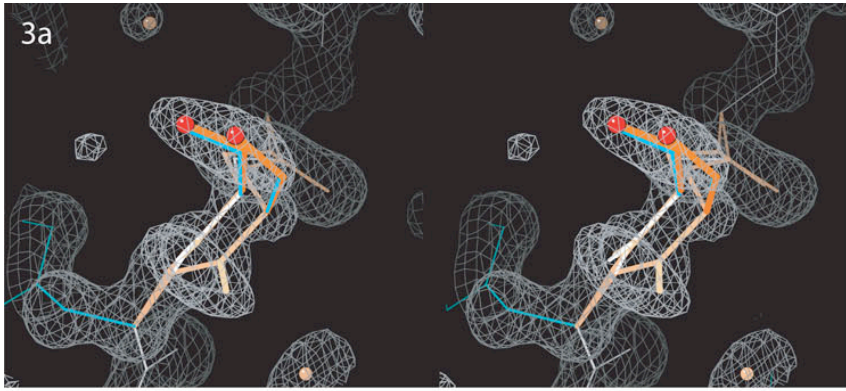


Figure 4: The BACKRUB tool in KiNG (Davis et al., 2004) was used to rebuild Ile A120 of 1MO0. (a) The original conformation had serious steric clashes (*pink spikes*) with the surrounding residues and occupied a negative peak in the difference density (*magenta*). (b) The *pt* rotamer has clashes on one side and a small cavity on the other. (c) The BACKRUB model (*peach/orange*) shifts Ile A120 into that empty space and establishes good packing contacts (*green and blue dots*) with its neighbors, as well as satisfying positive peaks in the original difference density (*green*).

Figure 4

